Muography as a new tool to study the historic earthquakes recorded in ancient burial mounds

Hiroyuki K.M. Tanaka[1,2], Kenji Sumiya[3], László Oláh[1,2]

[1]Earthquake Research Institute, The University of Tokyo, 1-1-1 Yayoi, Bunkyo, Tokyo 113-0032, Japan
[2]International Muography Research Organization (MUOGRAPHIX), The University of Tokyo, 1-1-1 Yayoi, Bunkyo, Tokyo 113-0032, Japan
[3]Graduate School of Informatics, Kansai University, 2-1-1 Ryozenji-cho, Takatsuki-shi, Osaka 569-1095, Japan

Abstract

Bidirectional muographic measurements were conducted at the Imashirozuka burial mound, Japan. The mound was built in the beginning of the 6th century as a megalithic tomb and was later collapsed after a landslide caused by the 1596 Fushimi Earthquake, one of the largest earthquakes that have occurred in Japan over last few centuries. The measurements were conducted in order to find evidence of this past disaster recorded in this historical heritage site. As a result, the vertical low-density regions were found at the top of the mound. These regions were interpreted as large-scale vertical cracks that caused the translational collapse process behind the rotational landslide that was already found in the prior trench-survey-based works. These results indicate that there was an intrinsic problem with the stability of the basic foundation of the Imashirozuka mound before the 1596 Fushimi Earthquake.

1. Introduction

By expanding our understanding of past large-scale natural disasters, such as tsunami, earthquakes and volcanic eruptions, future hazards can be extrapolated and estimated. However, modern scientific records of these natural disasters only, for the most part, cover events from the last couple of centuries, which have been recorded by scientific instruments only in limited regions throughout the world. On the other hand, geographical or topographical modifications are often physically recorded in the land surface as a result of such large-scale natural disasters, and correct methodologies can be deciphered to infer unknown details about these events. For example, a large-scale volcanic eruption usually creates a large volume pyroclastic flow, which later remains in the geological stratum as a sedimentation of volcanic products. By applying a geological dating technique to these past remnants of the eruptions, we can infer the timing and the magnitude of the past disasters. However, the geological timescale is largely different from that of human history, and the dating precision by these geochronological techniques is limited to an order of 100 years. On the other hand, historical studies often provide records that can be verified with yearly or sometimes, daily precision, depending on how far back the disaster occurred. Historical information is more straightforward regarding affected sites and the year or date of the disaster. For example, this information can come from literature, which describes destruction by earthquakes or repairs after earthquakes, providing valuable evidence for the location of earthquakes and the effects brought by these earthquakes. Therefore, if we can combine the historian's knowledge with the analysis results of these past disaster remnants, historical records become valuable information which can help to improve the accuracy of these geological dating techniques by developing into an iteration process. The derivation by scientists and engineers have been utilized as evidence of earthquakes and which are later incorporated by historian to evaluate the dates of the events, and vise versa.

Thus far, a combination of geological techniques and historical data have been applied to historically well-studied objects to fill the gaps in our understanding of the historical natural disaster record including tsunami (Daly et al., 2019; Dey et al. 2014), earthquakes (Korjenkov and Mazor, 2003; Guidoboni et al., 1994; Ambraseys et al. 1983) and volcanic eruptions (Elson and Ort, 2018). The data are exploited mostly by direct excavation of the historic site, and such anatomical techniques (similar in principle to dissecting bodies to directly view organs within human bodies) allow us to exploit regional, direct and detailed information; however, not all historical heritage sites can be accessible and modified in this way. For example, due to the cultural restriction, it is not always possible to conduct a trench survey to excavate the extant historical structures such as the ancient monuments or public buildings to obtain the geological knowledge about the past disaster remnants. Even when such a style of investigation is approved, the exploitable information is usually localized. Thus, there is a need for a non-invasive technique such as surface wave exploration, which would be conducted to provide a more overall picture of targeted structures to increase the possibilities of finding more physical evidence of past disasters.

Muography is a technique enabling us to "x-ray" gigantic (hectometric to kilometric) objects. The surface of the Earth is constantly bombarded with muons, particles that have decayed from cosmic rays arriving at the atmosphere from outside our solar system, and these particles can be utilized as probes for muography. After traversing targeted object, remnant muons are tracked with a particle detector located at lower elevations than the region of interest inside the target. The result is a pattern of the contrast in the density distribution inside the objects, which is projected on a 2-dimensional plane. Muography has been applied to image the internal structure of volcanoes (Tanaka et al. 2007; Tanaka et al., 2009; Lesparre et al., 2012; Tanaka et al., 2014; Olah et al., 2019), cultural heritages including Giza pyramids (Cheops and Chephren), Egypt, Prambanan temples, Indonesia, Mt Echia, Italy and Santa Maria del Fiore, Italy (Alvarez et al., 1970; Hanazato and Tanaka, 2016; Tanaka and Ohshiro, 2016; Morishima et al., 2017; Guardincerri et al. 2018; Cimmino et al. 2019), industrial plants (Tanaka, 2013), and other natural (Tanaka et al., 2011; Olah et al. 2012; Schouten, 2018) and man-made structures (Mahon et al. 2018). Prior works have focused on searching undiscovered chambers or the total weight of the heritage. Instead, in this work, we applied muography to study ancient earthquakes for the first time. We focused on the 1596 Fushimi Earthquake, one of the largest earthquakes that have occurred in Japan over last few centuries and examine whether the technique of muography can increase the possibilities of finding more physical evidence of past disasters recorded in historical heritage sites.

2. Observation

Imashirozuka, an imperial burial mound in Japan was chosen as a target of the current study. In Japan, imperial burial mounds have been well studied and a lot of knowledge has accumulated. For the current study, this type of the burial mound has the following advantages to study past earthquakes (Kamai et al., 2008). (A) The construction method of the imperial mound is well studied by historians and thus, even if the mound has been damaged by the past earthquakes, the original structure of the mound can be estimated. (B) The imperial mound was built as a stable object, and thus collapsed areas inside the mound would be likely to be records of past major earthquakes. (C) The imperial mounds are in general situated in the urban area. Therefore, the collapsed mounds can be used as an index to measure the past seismic disasters in urban areas long ago. (D) In the recent human's history, various kinds of embankments have been built, but its stability is discussed within the time scale of decades. The collapsed mounds offer us a unique opportunity of geotechnical discussions within a time scale of centuries. (E) The construction method of the mound was already well established when they were built. The mounds built in the same era used the same construction method and thus it is expected that the mechanical strength is the same. Therefore, the different collapsing conditions among different mounds located near each other could infer different ground conditions or different underwater conditions.

Imashirozuka is a keyhole-shaped imperial burial mound that was built in the beginning of the 6th century in Japan. This burial mound is situated on one of the most active faults in Japan, which is part of the Rokkou active fault system. This fault system caused the Great Hanshin Earthquake in 1995. In 1596, it is thought that this Rokkou active fault system and the next neighbor fault system called the Arima-Takatsuki tectonic line were activated at the same time, and one of the largest earthquakes in the last few centuries, Fushimi Earthquake, (Magnitude 7.25-7.75) occurred (Kamai et al., 2008). The total length of the Imashirozuka mound is 190 m and the height is 11-12 m. Although this burial mound was originally built in the triple-layered structure, the top layer collapsed after a landslide. The collapse occurred more extensively in the northern part of the mound. The level of damage depends, in general, on the ground motion during an earthquake, which itself depends on its magnitude and distance from the site. This extensive collapse is probably due to the existence of the Ai fault line, a part of the Rokkou active fault system, is located closer to the northern part of the mound. Currently, Imashirozuka mound consists of a base layer made of high bulk density sandy clay (a soil particle density of 2.6 gcm^{-3} with a porosity of 52%), and a middle layer made of lower bulk density granules (a soil particle density of 2.6-2.8 gcm^{-3} with a porosity of 76%) (Kamai et al., 2008). The s-velocity structure observed in the base layer was faster (harder) in comparison to the middle layer (Kamai et al., 2008). For the purpose of the archaeological studies, 6 trenches were excavated and landslide remnants were observed in many of these trenches. The burial mound was originally surrounded by a double moat, but most of this moat was buried in the past, and only a part of it currently remains. The landslide deposits originated from the sediments in the moat were dated, and the results were 1420-1510 AD with a method of the C^{14} dating (Sangawa and Miyazaki 2001). Since it is known that Fushimi Earthquake occurred in 1596, this burial mound collapse was thought to have been triggered by this earthquake (Sangawa and Miyazaki 2001).

The top view of the landslides generated by the 1596 Fushimi Earthquake is shown in Figure 1 (Kamai et al., 2008). The results of the trench survey indicated that most of the landslide types were represented by a combination of translational and rotational landslides (Kamai et al., 2008). Movement was inferred with the following sequence: 1. the landslide mass moved near horizontally for a few meters, 2. the transported landslide mass reached the inner moat, 3. the landslide mass slid down and shifted from translational to rotational landslide mode. Conversely, it was found that an exceptionally large-scale rotational landslide occurred in the north side of the round-shaped section of the burial mound. Whether the burial mound deformation related to this rotational slide is connected to the translational landslide had continued to be a mystery. The purpose of this work was to examine whether muographically found evidence can be used to address this question.

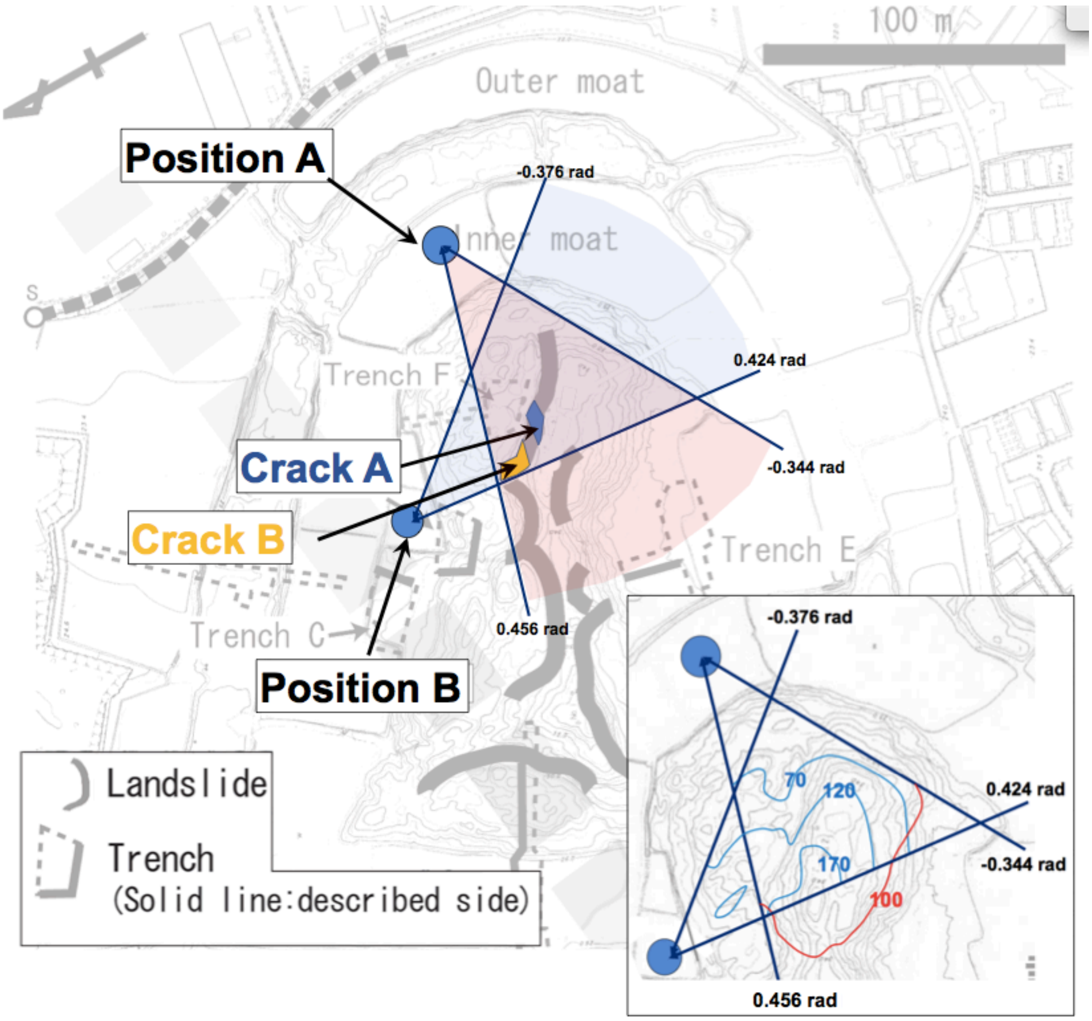

Figure 1. Top view of Imashirozuka burial mound. Positions A and B indicate the locations of the detectors for the current bidirectional muographic observations. The shaded areas in red and blue indicate the viewing angle of each measurement. The inset shows the geometrical information of the mound. The red and blue solid curves respectively indicate the cross sections of the mound at given elevation angles from Positions A and B. The red and blue numbers indicate the elevation angles in units of mrad.

In Figure 2, the cross-sectional view of the mound sliced along Line F in Figure 1 is shown. This structure has been modeled based on the trench surveys conducted in 2008 (Kamai et al. 2008). Original surface of the mound (dashed lines in Figure 2) that was estimated from the past archaeological studies, was lost by the landslide triggered by the 1596 Fushimi earthquake. The red lines indicate the slip surface of the landslide and at the top of this surface, the existence of near-vertical cracks was expected. From these trench surveys, the region indicated between the red lines and the solid black lines in this figure was interpreted as the landslide mass, and displayed lower density than the other part of the mound and thus, it was expected that muons could penetrate more in this region (in particular at the top of this region).

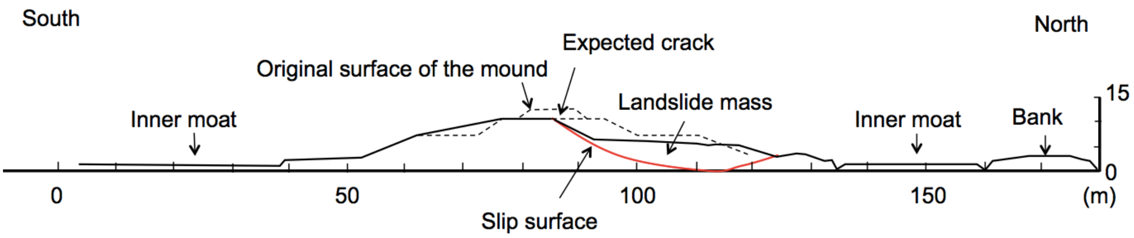

Figure 2. Cross-sectional view of the mound along Line F in Figure 1. The dashed lines indicate the original surface of the mound, and the red lines indicate the slip surface of the landslide triggered by the 1596 Fushimi earthquake. The authors drew this image based on the work done by Kamai et al. (2008).

Mechanical fractures within rock and soil produce a significant amount of interparticle space and these fractured zones are detected as lower-density-regions in muographic images (Tanaka and Muraoka, 2013, Carbone et al. 2014). Likewise, when a landslide occurs, various processes influence changes in the density distribution inside a burial mound. When a crack is generated in the burial mound, the density is reduced along the crack. If a large-scale collapse occurs, the collapsed landslide mass will contain a lot of inter-particle voids, and the density will be reduced. If the geometrical arrangement is altered between the high-density base layer and lower density middle layer due to the ground motion such as a fault slip, the overall density distribution will be altered accordingly. All of these variations can be imaged with muography.

3. Method

Bidirectional muographic measurements were conducted at the Imashirozuka burial mound site so that the resultant images could be used for 3-dimensional interpretation of the internal structure of the circular section of the mound. In particular, one of the detector positions of the current bidirectional measurements were chosen on the northern side of the round-shaped section (Position B) so that the area where the extensive collapse occurred could be more closely observed. The positions chosen for the current measurement are shown in Figure 1. The first measurement of the Imashirozuka mound started at Position A on September 21, 2019. The data were taken for 40 days, and subsequently the detector was moved to Position B to collect the data for another period of approximately one month.

The detector employed for the current measurement was the multi-wire proportional chambers (MWPC) based muographic observation system (MMOS) that consists of 6 layers of MWPCs and lead plates with a total thickness of 10 cm. A detailed description of the MMOS can be found in elsewhere (Olah et al. 2018), and thus only the main features are briefly introduced here. In between each of the MWPC, a 2-cm thick lead plate accommodated in a 4 mm-thick-stainless steel case is inserted, thus the total thickness of these radiation shields is equivalent to ~130 gcm^{-2}. These radiation shields function as an absorber or a scatterer of low energy background particles that include muons or other elecromagnetic particles. The wire distances were designed to be 12 mm in MWPC detectors to provide a fair positional resolution of approx. 4 mm even if lead plates were applied between the MWPCs (Varga, D. et al., 2015; Varga, D. et al., 2016; Olah, L. et al., 2018). The angular resolution of 1.5 meter-length tracking system was approx. 2.7 mrad (Olah, L. et al., 2018). Only the straight trajectories throughout 6 detectors are employed and recorded as muons. The penetration of muons and electrons were simulated in GEANT4 simulation framework (Olah, L. et al., 2019). The analysis cut on the goodness of track fit was set to 1.5 to suppress the penetration of muons down to 10 % those had the energy of < 1 GeV. This simulation study showed that the electromagnetic component did not create signal in the MMOS. In the current measurements, the total weight of the MMOS was 600 kg including the case, batteries and gas bottle. The total power consumption of the detector was ~30W, and the six 400-Wh lithium-ion batteries loaded into the case allowed us the continuous operation for 80 hours, and the recurrent charging and replacements of the batteries further extended the time of the continuous operation. The flow rate of the Ar-CO_2 gas mixture (Ar:80, CO_2:20) through the chambers was 1–2 liters per hour to enable continuous operation for a few months with a standard 40L type (6,000 litters) gas bottle. The casters attached to the bottom of the case facilitated movements of the detector around the mound. Moisture absorbent boxes were equipped inside the box in order to retain the humidity at a constant level around the MWPCs. The size of the active area of the detector was 80 x 80 cm^2, and the distance between the uppermost and lowermost stream detectors were 150 cm. The recorded muon tracks were stored and the numbers of muon counts were directionally sorted out into a matrix with an angular binning width of 8 mrad x 8 mrad. As is indicated in Figure 1, the azimuthal viewing angle was +/-500 mrad, however, due to the smaller geometrical acceptance for larger angles, only the data within +/-400 mrad were used. The detector cost was ~60k US dollars, but the operational cost was suppressed to a few thousand US dollars for entire operation including the transportation, human resources for battery replacements and data download.

Since the current target size is an order of 100 m, the following simplified analytical expression can be applied for derivation of the relative density variations inside the target volume because the muon's cutoff energy (the minimum energy of the muons that can escape from the target volume) is much lower than the critical energy, 708 GeV in SiO_2, the continuous ionization process is the main energy loss process (Tanaka and Ohshiro, 2016).

$$I_0/I_1=(X_0/X_1)^{-\gamma}, \quad (1)$$

where I_0 and I_1 is the remnant muon flux after passing through different densimetric thickness of rock X_0 and X_1. The Greek symbol, γ, is the zenith-angular dependent index of the power low of the integrated muon spectrum within 50-200 GeV. In this work, only the "relative muon flux" was used for discussions of the density contrast inside the mound. The obtained matrix has been normalized by the azimuthal distribution of the open-sky flux so that the azimuthally angle-dependent acceptance has been canceled in the image.

4. Results

Figure 3 shows the muographic image (Image A) taken at Position A that is indicated in Figure 1. Corresponding azimuthal angles (-0.344 rad - 0.456 rad) are shown in Figure 1. The distance between the detector and the peak of the mound was 70 m, and thus the elevation angle of the mound peak was ~110 mrad (~6 degrees). Since the aspect ratio of the mound, i.e., the ratio of its width to its height (10:1) was large, the matrix was not re-binned in the elevational direction, but was re-binned in 40 mrad in the azimuthal direction in order to increase the statistics. The total number of muons collected at Position A in the elevational-angle-region below 180 mrad was 76,682. The number of muons recorded in the bins at an azimuthal angle of 0 ranged from 30 to 500, depending on the elevational angle. The data were normalized to the azimuthal distribution of the open-sky muon tracks that was unaffected by the existence of the mound, which corresponds to the elevational region between 300 and 360 mrad in order to derive the "relative muon flux". The bottom right green-colored region in Figure 3, where the number of muons was counted less than other regions corresponds to the direction because in the positive azimuthal angular region at Position A, the rectangular section of the mound provided the additional path length for muons that arrived at lower elevation angles. It was expected that the region around landslide headscarps (arc-shaped lines in Figure 1) had cracks, and thus the average density along these cracks was significantly lower than the density around these. This density reduction effect is maximized in muographs when the muon's ray path is parallel to these cracks. From Position A, this direction corresponds to the azimuthal angular range between 200 mrad and 300 mrad (see the position indicated by "Crack A" in Figure 1).

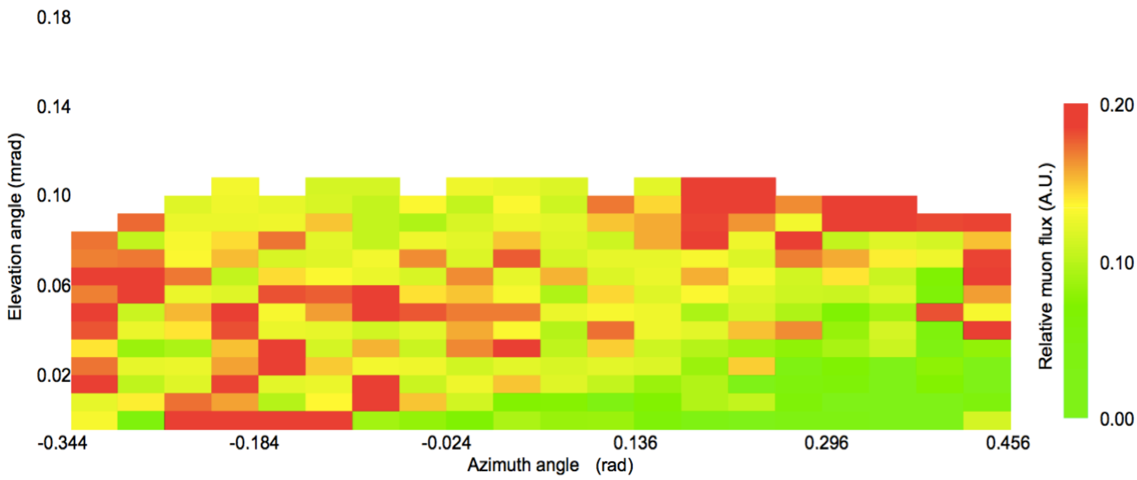

Figure 3. Angular distribution of the relative muon flux, as was observed from the measurement at Position A. The horizontal and vertical bin widths are respectively 40 mrad and 8 mrad. The azimuthal distribution of the relative muon flux was normalized to the total number of muons counted at each elevation angle.

Figure 4 shows the azimuthal distribution of the relative muon flux at shallow depths (at elevation angles of 108 mrad (Figure 4A) and 100 mrad (Figure 4B)). The solid lines are the expected muon flux. These lines were drawn based on the geometrical thickness of the mound along the muon paths (Figure 1) by assuming the uniform density distribution inside the mound. In these three images, the following three features can be found. (A) Overall, the excessive flux of muons was observed in the positive azimuthal angle region. This indicates that the average density in the positive azimuthal angle region is lower than that in the negative angle region. An overall density variation between them is 10-20%. (B) A strongly excessive muon flux can be found in the azimuthal angle region between 176 mrad and 296 mrad in Figures 4A and 4B. The statistical significance was more than 4σ. (C) In Figures 4A, there is also a low-density region within the azimuthal angle range between 296-456 mrad. The position of this low-density region corresponds to that of Trench F (dotted lines in Figure 1). From (A) and (B), it was inferred that a large almost vertical crack exists in the shallow region, however its existence was not clear when it's deeper than 2 m because of the effect of overlapping the rectangular-shaped background mound (see the green-colored area at the right bottom region of Figure 3). The density variations of this possible crack were 20-30% in comparison to the average density of the other part of the mound. The crack width was 80-120 mrad that was equivalent to 6-8 m when considering the distance between the detector and Crack A of 70 m.

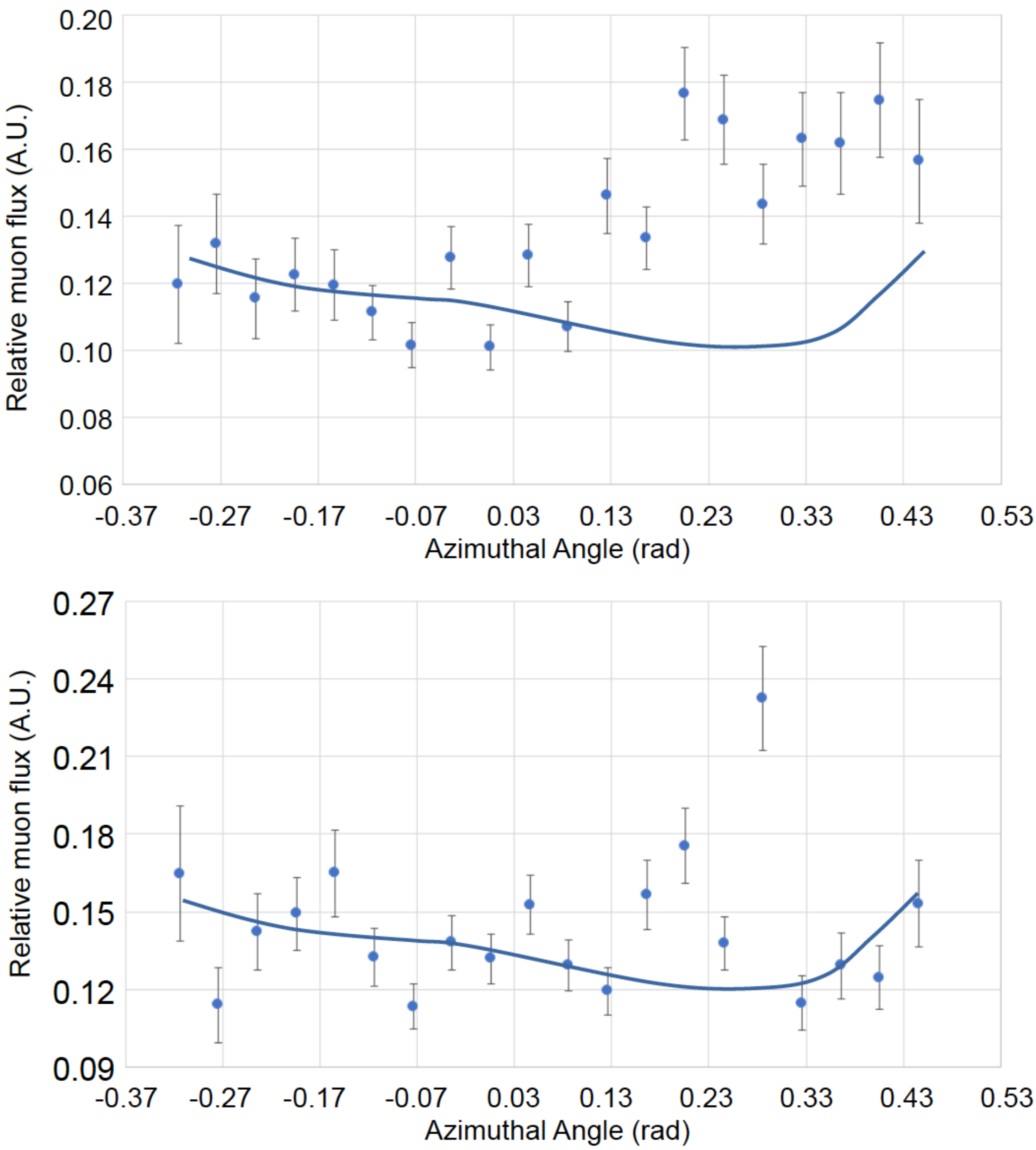

Figure 4. Azimuthal distribution of the relative muon flux for elevation angles of 100 mrad (top) and 92 mrad (bottom). The solid curves indicate the expected horizontal muon flux variations.

Crack A was not parallel to the muon's ray path at Position B (Figure 1), however, Crack B was parallel to those in the azimuthal angle range between 300-420 mrad. Therefore, it was expected that the similar structure to Crack A would be observed in this angular region. Figure 5 shows the muographic image (Image B) taken at

Position B. Since the distance to the mound peak (50 m) was closer at Position B, the spatial resolution at the mound peak was improved for a given angular resolution of the tracker. The total number of muons collected at Position B in the elevational-angle-region below 180 mrad was 15,214. The number of muons recorded in the bins at an azimuthal angle of 0 ranged from 15 to 100, depending on the elevational angle. The data were normalized to the azimuthal distribution of the muon tracks recorded within the elevational range between 300 and 360 mrad in order to derive the "relative muon flux". Corresponding azimuthal angles (-0.376 rad - 0.424 rad) are shown in Figure 1.

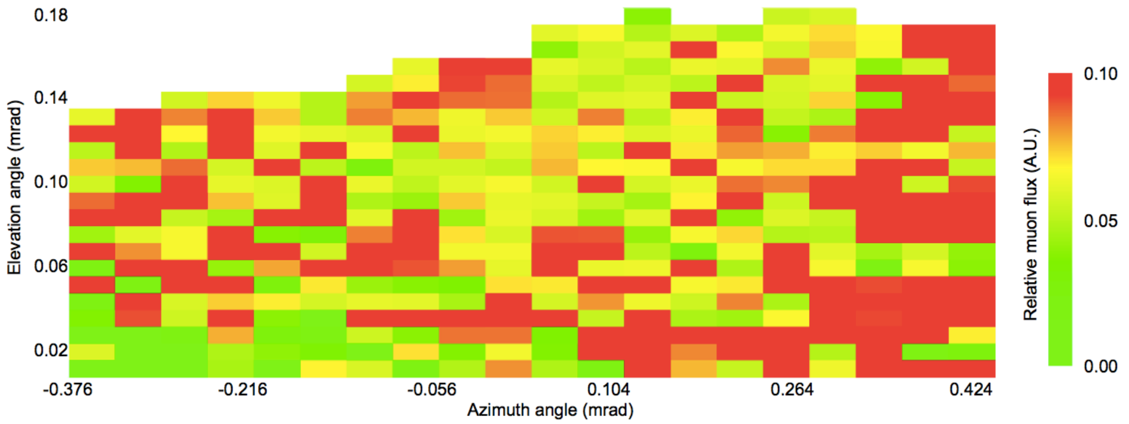

Figure 5. Angular distribution of the relative muon flux observed at Position B. The horizontal and vertical bin widths are respectively 40 mrad and 8 mrad. The azimuthal distribution of the relative muon flux was normalized to the total number of muons counted at each elevation angle.

In Figure 6, the azimuthal distribution of the relative muon flux for elevation angles of 68 mrad - 172 mrad are shown. In these images, the excessive muon flux was found within the azimuthal angle range between 264-424 mrad. The statistical significance was overall more than 1σ, but was increased to 2-3σ in the shallower region of the mound. This low-density region was interpreted as the combination of Cracks A and B, and it was found that the vertical extent of the crack was much deeper than what could be seen in Image A. The crack width was at least 80-160 mrad that was equivalent to 4-8 m when considering the distance between the detector and Crack B. The reddish region in Figure 5 that can be seen on the left side of Crack B indicates low-density collapsed landslide mass, with a mixture of the remnant of the past excavation at Trench F.

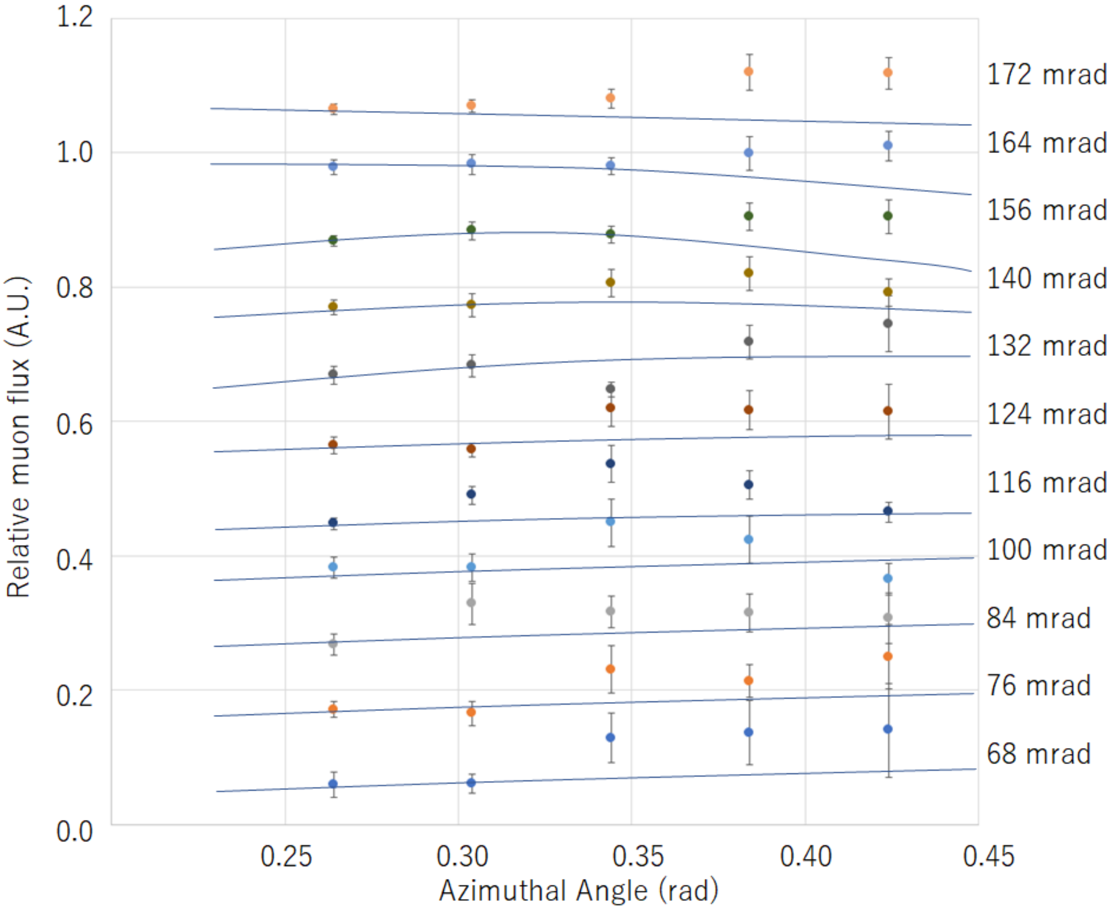

Figure 6 Azimuthal distribution of the relative muon flux for various elevation angles. The solid curves indicate the expected horizontal muon flux variations. The relative muon flux values were multiplied for better visualization.

5. Discussion

From the bidirectional muographic images taken in the current measurements, the following interpretations were derived.

The vertical low-density regions at the top of the mound in Images A and B show that there is a large-scale vertical crack behind Landslide headscarp. The widths of these vertical cracks were both 4-8 m thus it is reasonable to assume they are associated with the same scarp.

In conclusion, the following picture was proposed. In prior trench-survey-based works, most of the landslides that deformed this burial mound structure were found to have been caused by a translational process. On the other hand, there was an exceptionally large-scale rotational slide was found in the north region of the round-shaped section of the mound, and the stone chamber was deformed and destroyed by this collapse process. However, in the current muographic observations, a large-scale vertical crack was discovered at the top of the round-shaped section, and it was found that the burial mound deformation that connected to the translational collapse process also occurred behind this rotational landslide. These data indicate that there was an intrinsic problem with the stability of the basic foundation of the Imashirozuka mound before the 1596 Fushimi Earthquake. Changes in the foundation as a response to shaking from the earthquake may have produced this large-scale burial mound collapse.

The burial mound seems to have a robust structure, more stable against earthquakes than slender buildings like clock towers. However, a number of the ancient burial mounds throughout Japan have collapsed from earthquakes and many modern buildings are now built upon them. A small fraction has survived since early times, however, they do not always indicate the earthquake-free sites. They represent an example of the final designs of ancient Japanese construction since they have remained even after having experienced a number of destructive earthquakes.

The technique of muography, which can probe seismically damaged ancient mounds is similar to medical radiography which seeks to find the position, formation, and size of the fractured zone inside the human body. In general, it is difficult to understand the extent of damage, for example, of a patient's external wound without also understand what is happening inside the body. The outside structure of ancient mounds is similar. The surface of them has usually been naturally or artificially eroded with added vegetation covering the shape during a long period of time it has existed. However, the inside is more intact. For this reason, the trench survey technique (physically digging a trench into the structure) to understand the "inside" can reveal valuable data. However, similar to the manner in which x-ray photographs are usually applied to a diagnosis before surgery is considered, muography is a more convenient and noninvasive technique to effectively understand the overall inside structure to assess the effect of time and natural disasters on the structure as a whole.

The current proof of concept measurement has attempted to show whether the technique of muography increases the possibilities of finding more physical evidence related to past earthquakes by selecting the Imashirozuka mound as an example. Obviously, the specific earthquake damage of each burial mound is unique and cannot be generalized. Its response depends not only on its material properties of the mound including its mechanical properties of its foundations (strength and rigidity), but also on the ground motion during an earthquake. Surveying and mapping various mounds that are thought to be affected by the earthquake will provide a valuable data for us to verify and sort out the factors that caused the damage.

Not only Imashirozuka mound but also other various burial mounds including the Mishima mound group and the Kobo mound group are concentrated along the Rokkou active fault system and its next neighbor Arima-Takatsuki tectonic line. The current muographic results suggest that a combination of muography and the techniques of trench survey or other conventional geophysical techniques can contribute towards the construction of a more comprehensive understanding of the seismic response and deformation of each burial mound. The characteristics of muography would allow researchers to conduct an investigation of several sites quickly and efficiently to grasp the general trend of the ensemble of these sites. Incorporating the muography visualization technique into engineering expertise and in conjunction with historical comparanda would utilize a new potential: by acquiring this new, valuable data from these ancient burial mounds in Japan and other similar sites worldwide, we would increase our ability to tackle future challenges of natural disaster preparation.

Acknowledgements

The authors acknowledge Toshitaka Kamai for valuable discussions about the current muographic observation results. The authors also acknowledge Takefumi Hayashi for his coordination and support the current measurements, Fumitaka Yoneda & Chikara Inoue for their valuable archaeological advice, Ichiro Kanegae for provision of past excavation research materials of Imashirozuka mound, and Masao Uchida for his support as a chief administrator of Imashirozuka park. The authors acknowledge two anonymous referees for their valuable suggestions.

References

Alvarez, L. W., Anderson, J. A., El Bedwei, F., Burkhard, J., Fakhry, A., Girgis, A., Goneid, A., Hassan, F., Iverson, D., Lynch, G., Miligy, Z., Moussa, A. H., Sharkawi, A., and Yazolino, L.: Search for hidden chambers in the pyramid, Science, 167, 832– 739, doi:10.1126/science.167.3919.832, 1970.

Ambraseys NN., Banda E., Irving J., Mallard D., Melville C., Morse T., Muir-Wood R., Munoz D., Serva L., Shilston D., Surinach E., Vogt J.: Notes on Historical Seismicity. Bull. Seismol. Soc. Am. 73(6), 1917–1920, 1983.

Carbone, D., Gibert, D., Marteau, J., Diament, M., Zuccarello, L., and Galichet, E.: An experiment of muon radiography at Mt. Etna (Italy), Geophys. J. Int., 196, 633–643, 2013.

Cimmino, L., Baccani, G., Noli, P., Amato L., Ambrosino, F., Bonechi, L., Bongi, M., Ciulli, V., D'Alessandro, R., D'Errico, M., Gonzi, S., Melon, B., Minin, G., Saracino, G., Scognamiglio, L., Strolin P., Viliani, L.: 3D Muography for the Search of Hidden Cavities, Scientific Reports 9, 2974, 2019.

Daly, P., Sieh, K., Yew Seng, T., McKinnon, EE., Parnell, AC., Ardiansyah, R., Feener, M., Ismail, N., Nizamuddin, Majewski J.: Archaeological evidence that a late 14th-century tsunami devastated the coast of northern Sumatra and redirected history, PNAS, 116 (24) 11679-11686, 2019

Dey, H., Goodman-Tchernov, B., Sharvit, J.: Archaeological evidence for the tsunami of January 18, A.D. 749: a chapter in the history of Early Islamic Qaysariyah (Caesarea Maritima), Journal of Roman Archaeology, 27, 357-373, 2014.

Elson, M., Ort, M.H.: Archaeological Volcanology, The Encyclopedia of Archaeological Sciences. Edited by Sandra L. López Varela. John Wiley & Sons, Inc., 1-5, 2018.

Guardincerri E., Bacon JD., Barros N., Blasi C., Bonechi L., Chen A., D'Alessandro R., Durham JM., Fine M., Mauger C., Mayers G., Morris C., Newcomer FM., Okasinski J., Pizzico T., Plaud-Ramos K., Poulson DC., Reilly MB., Roberts A., Saeid T., Vaccaro V., Van Berg R.: Imaging the dome of Santa Maria del Fiore using cosmic rays, Philos. Trans. A Math. Phys. Eng. Sci. 377 (2137) 20180136, 2018. doi:

10.1098/rsta.2018.0136.

Guidoboni, E., Comastri, A., Traina G., Catalogue of Ancient Earthquakes in the Mediterranean Area up to the 10th Century, Istituto Nazionale di Geofisica, Rome, 1994.

Hanazato, T., Tanaka, HKM.: Inspection of the internal structure of the UNESCO-World Heritage with cosmic rays, Isotope News, 741, 60-64, 2016.

Kamai, T., Sangawa, A., Shuzui, H.: Landslides on Ancient Burial Mounds Induced by the 1596 Keicho-Fushimi Earthquake, Jour. Japan Soc, Eng. Geol., 48, 6, 285-298, 2008.

Korjenkov, AM., Mazor E.: Archaeoseismology in Mamshit, Southern Israel, cracking a millennia-old code of earthquake preserved in ancient ruins, Archäologischer Anzeiger, 2, 51-82, 2003.

Lesparre, N., Gibert, D., Marteau, J., Komorowski, J.-C., Nicollin, F., and Coutant, O.: Density muon radiography of La Soufriere of Guadeloupe volcano: comparison with geological, electrical resistivity and gravity data, Geophys. J. Int., 190, 1008–1019, 2012.

Mahon D., Clarkson A., Gardner S., Ireland D., Jebali R., Kaiser R., Ryan M., Shearer C., Yang G.: First-of-a-kind muography for nuclear waste characterization, Philos. Trans. A Math. Phys. Eng. Sci. 377 (2137) 20180048, 2018. doi: 10.1098/rsta.2018.0048.

Morishima K., Kuno M., Nishio A., Kitagawa N., Manabe Y., Moto M., Takasaki F., Fujii H., Satoh K., Kodama H., Hayashi K., Odaka S., Procureur S., Attié D., Bouteille S., Calvet D., Filosa C., Magnier P., Mandjavidze I., Riallot M., Marini B., Gable P., Date Y., Sugiura M., Elshayeb Y., Elnady T., Ezzy M., Guerriero E., Steiger V., Serikoff N., Mouret JB., Charlès B., Helal H., Tayoubi M.: Discovery of a big void in Khufu's Pyramid by observation of cosmic-ray muons, Nature, 552(7685), 386-390, 2017. doi: 10.1038/nature24647

Olah L., Tanaka, HKM., Ohminato T., Hamar G., Varga D.: Plug Formation Imaged

Beneath the Active Craters of Sakurajima Volcano With Muography, Geophys. Res. Lett., GL084784, 2019. doi.org/10.1029/2019GL084784.

Olah, L., Barnaföldi, G. G., Hamar, G., Melegh, H. G., Surányi, G., and Varga, D.: CCC-based muon telescope for examination of natural caves, Geosci. Instrum. Method. Data Syst., 1, 229–234, doi:10.5194/gi-1-229-2012, 2012.

Olah L., Tanaka HKM., Ohminato T., Varga D.: High-definition and low-noise muography of the Sakurajima volcano with gaseous tracking detectors, Sci Rep. 8(1), 3207, doi: 10.1038/s41598-018-21423-9, 2018.

Sangawa, A., Miyazaki, Y.: Traces of Landslides found in Imashirosuka mound, 18th meeting of Japan Society for Scientific Studies on Cultural Property, 24-25, 2001.

Schouten, D.: Muon geotomography: selected case studies, Philos. Trans. A Math. Phys. Eng. Sci. 377 (2137) 20180061, doi: 10.1098/rsta.2018.0061, 2018.

Tanaka, H. K. M., Nakano, T., Takahashi, S., Yoshida, J., Takeo, M., Oikawa, J., Ohminato, T., Aoki, Y., Koyama, E., Tsuji, H., and Niwa, K.: High resolution imaging in the inhomogeneous crust with cosmic-ray muon radiography: The density structure below the volcanic crater floor of Mt. Asama, Japan, Earth Planet. Sc. Lett., 263, 104–113, 2007.

Tanaka, H. K. M., Uchida, T., Tanaka, M., Takeo M., Oikawa J., Ohminato T., Aoki Y., Koyama, E., Tsuji H.: Detecting a mass change inside a volcano by cosmic-ray muon radiography (muography): First results from measurements at Asama volcano, Japan, Geophys. Res. Lett., GL039448, doi.org/10.1029/2009GL039448, 2009.

Tanaka, H. K. M., Miyajima, H., Kusagaya, T., Taketa, A., Uchida, T., and Tanaka, M.: Cosmic muon imaging of hidden seismic fault zones: Raineater permeation into the mechanical fracture zone in Itoigawa-Shizuoka Tectonic Line, Japan, Earth Planet. Sc. Lett., 306, 156–162, 2011.

Tanaka H.K.M., Kusagaya T., Shinohara H., Radiographic visualization of magma dynamics in an erupting volcano, Nat Commun. 10, 5, 3381, doi: 10.1038/ncomms4381, 2014.

Tanaka, H. K. M.: Development of stroboscopic muography, Geosci. Instrum. Method. Data Syst., 2, 41–45, doi:10.5194/gi- 2-41-2013, 2013.

Tanaka, H. K. M., Ohshiro, M.: Muographic data analysis method for medium-sized rock overburden inspections, Geosci. Instrum. Method. Data Syst., 5, 427–435, doi:10.5194/gi-5-427-2016, 2016.

Tanaka H. K. M., Muraoka, H.: Interpreting muon radiographic data in a fault zone: possible application to geothermal reservoir detection and monitoring, Geosci. Instrum. Method. Data Syst., 2, 145–150, https://doi.org/10.5194/gi-2-145-2013, 2013.

Varga D., Gál, Z., Hamar G., Molnár, J.S, Oláh, E. and Pázmándi, P.: Cosmic muon detector using proportional chambers, European Journal of Physics, 36, 065006, 2015.

Varga D., Nyitrai, G., Hamar, G., Oláh, L., High Efficiency Gaseous Tracking Detector for Cosmic Muon Radiography, Advances in High Energy Physics, 1962317, https://doi.org/10.1155/2016/1962317, 2016.